Physics Letters B 830 (2022) 137144

Contents lists available at ScienceDirect

Physics Letters B

www.elsevier.com/locate/physletb

Mirror symmetry at mass $A = 54$: $E4$ effective charges near doubly magic ^{56}Ni

D. Rudolph [a,*], B. Blank [b], J. Giovinazzo [b], T. Roger [c], H. Alvarez-Pol [d], A. Arokia Raj [e], P. Ascher [b], M. Caamaño-Fresco [d], L. Caceres [c], D.M. Cox [a], B. Fernández-Domínguez [d], J. Lois-Fuentes [d], M. Gerbaux [b], S. Grévy [b], G.F. Grinyer [f], O. Kamalou [c], B. Mauss [g,1], A. Mentana [e,2], J. Pancin [c], J. Pibernat [b], J. Piot [c], O. Sorlin [c], C. Stodel [c], J.-C. Thomas [c], M. Versteegen [b]

[a] Department of Physics, Lund University, SE-22100 Lund, Sweden
[b] Centre d'Etudes Nucléaires de Bordeaux Gradignan, UMR 5797 CNRS/IN2P3 – Université de Bordeaux, F-33175 Gradignan Cedex, France
[c] Grand Accélérateur National d'Ions Lourds, CEA/DRF-CNRS/IN2P3, F-14076 Caen Cedex, France
[d] IGFAE and Dpt. de Física de Partículas, Universidade de Santiago de Compostela, E-15758 Santiago de Compostela, Spain
[e] Instituut voor Kern- en Stralingsfysica, KU Leuven, B-3001 Leuven, Belgium
[f] Department of Physics, University of Regina, Regina, Saskatchewan S4S 0A2, Canada
[g] RIKEN Nishina Center, Wako, Saitama 351-0198, Japan

ARTICLE INFO

Article history:
Received 1 February 2022
Received in revised form 14 April 2022
Accepted 29 April 2022
Available online 5 May 2022
Editor: D.F. Geesaman

Keywords:
^{54}Ni
Nuclear shell model
Isospin symmetry
Electromagnetic decay
$E4$ transition
Effective charges

ABSTRACT

Proton-emission branches of the 10^+ isomer in the $T_z = -1$ nucleus ^{54}Ni have been imaged with the active target and time projection chamber (ACTAR TPC) in an experiment conducted at the Grand Accélérateur National d'Ions Lourds (GANIL). The completed decay scheme allows derivation of the reduced transition strengths, $B(E2; 10^+ \rightarrow 8^+)$ and $B(E4; 10^+ \rightarrow 6^+)$, for the two competing γ-ray transitions. By means of a comparison with their well-known 'mirror transitions' in $T_z = +1$ ^{54}Fe, and aided by a variety of shell-model calculations in the fp model space, effective charges for $E4$ transitions near $N = Z$ ^{56}Ni can be deduced: $\varepsilon_\pi \approx 1.40$ and $\varepsilon_\nu \approx 0.30$. Mirror-energy differences are explored with various shell-model interactions and isospin-symmetry breaking terms.

As a consequence of the approximate charge symmetry of the nuclear force, nearly identical level structures and decay pattern are expected for pairs of mirror nuclei. These are nuclei with neutron and proton numbers reversed. Differences in energies and decay characteristics of levels with the same spin and isospin in mirror nuclei arise primarily from various contributions of the Coulomb energy, which breaks isospin symmetry. Comprehensive and unequivocal experimental information on energies, spins, parities, *and* decay branches are mandatory for reliable assessments of isospin-symmetry breaking terms within, for instance, the shell-model framework. Combined experimental and theoretical efforts, in the lower fp shell between ^{40}Ca and ^{56}Ni in particular, have been very successful and have shed light on isospin-breaking phenomena in a detailed way [1–6].

Often populated by nucleon removal reactions from relativistic radioactive beams, both an increasing number and increasingly exotic mirror pairs have come into experimental reach (see, e.g., Refs. [7–9] and references therein). From these studies, questions arise as to how to extend isospin non-conserving interactions of *nuclear* origin [5] into the upper fp shell, thus beyond ^{56}Ni, and whether or not analogue states are sensitive to weak binding, i.e., coupling to the continuum [10]?

In case lifetimes measurements of analogue states are feasible, it is possible to study and derive effective isoscalar and isovector charges, which relate to the effective multipole operators used to predict electromagnetic properties. This has been possible using fully-aligned five-hole states in the isospin $T_z = \pm 1/2$, $A = 51$ mirror system [11], providing $E2$ effective charges consistent with

* Corresponding author.
E-mail address: Dirk.Rudolph@nuclear.lu.se (D. Rudolph).
[1] Present address: CEA, DAM, DIF, F-91297 Arpajon, France.
[2] Present address: Dipartimento di Fisica, Università degli Studi di Pavia, I-27100 Pavia, Italy.

https://doi.org/10.1016/j.physletb.2022.137144

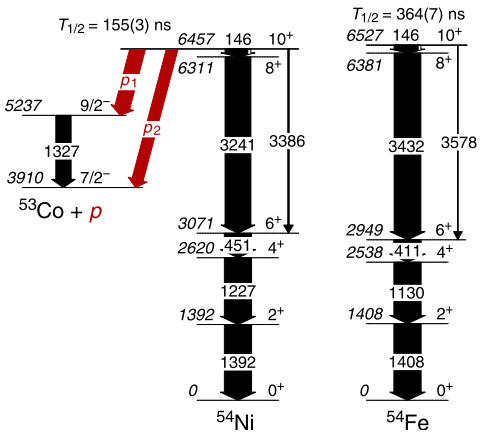

Fig. 1. Decay scheme of the 10^+ isomer in ^{54}Ni following the recently established proton-emission branch, p_2, into the ground state of ^{53}Co [13]. The corresponding decay scheme of the 10^+ isomer of the mirror nucleus ^{54}Fe [15,19] is shown to the right. Energy levels are in keV, and the widths of the arrows correspond to the relative yields of the decays, including internal conversion for the 146-keV transitions (open area of the arrows).

long standing predictions for $N \approx Z$ nuclei. A recent, similar study of decay properties of isomeric states near ^{100}Sn provided consistent values [12]. With the complete decay scheme of the core excited 10^+ isomer in ^{54}Ni established [13], the mass $A = 54$ mirror pair [14] now allows to investigate $E4$ effective charges, and also to contribute to the questions raised earlier.

Most of the currently available information on ^{54}Ni and its mirror nucleus ^{54}Fe is summarized in the most recent mass $A = 54$ evaluated nuclear structure data file [15]. In brief, ground-state β^+ decay of ^{54}Ni was identified with an element-selective laser ion source providing a low-energy secondary ^{54}Ni beam following production via the reaction ^{54}Fe(^{3}He,3n) [16]. A consistent ^{54}Ni ground-state decay half-life was measured following intermediate-energy fragmentation of ^{78}Kr and event-by-event isotope identification shortly after [17]. The $6^+ \rightarrow 4^+ \rightarrow 2^+ \rightarrow 0^+$ yrast cascade, governed by $\nu(f_{7/2})^{-2}_{0,2,4,6}$ wave-function partitions, was established by an in-beam γ-ray study. The ^{54}Ni level energies, together with the corresponding ones in the mirror nucleus ^{54}Fe, were assessed in terms of isospin-symmetry [18]. A 10^+ isomer in ^{54}Ni, expected as partner of the well-known 10^+ isomer in ^{54}Fe [15,19], was observed following population via fragmentation of a ^{58}Ni beam at relativistic energy [14]. The decay schemes of these mirror isomers are illustrated in Fig. 1. Next to extended information on isospin-symmetry breaking terms of effective interactions [14], that experiment provided indirect evidence for $\ell = 5$ proton radioactivity connecting this 10^+ isomer with the $9/2^-$ yrast state of ^{53}Co at 1327 keV excitation energy (p_1 in Fig. 1). Furthermore, isospin-symmetry arguments and quantum tunneling estimates indicated that an $\ell = 7$ proton-emission branch into the $7/2^-$ ground state of ^{53}Co (p_2 in Fig. 1) should exist as well, and with a yield comparable with p_1 [14]. In fact, a full isospin-symmetry assessment of the decay of the 10^+ isomers in the $A = 54$, $T_z \pm 1$ mirror pair was pending the direct measurement of that decay branch.

In an attempt to identify the proton branch p_2 with the help of a recoil-shadow set-up and production via fusion-evaporation reactions, the probability of populating ^{54}Ni in the 10^+ isomeric state was found to be too low [20]. In the present experiment, a substantial number of ^{54}Ni nuclei, in the 10^+ isomeric state, were produced by intermediate-energy fragmentation of an intense ^{58}Ni primary beam. Identified event-by-event, ^{54}Ni nuclei were stopped inside a novel time-projection chamber (ACTAR TPC [21,22]), which took four-dimensional pictures of $\approx$ 3000 proton-emission events [13]. From this data set, competing electromagnetic and proton-emission decay strengths can be derived, using $T_{1/2}(10^+) = 155(3)$ ns based on the present [13] and previous [14] measurements.

The ACTAR TPC experiment and subsequent data analysis are detailed in Refs. [13,23]. In brief, the experiment was conducted at the Grand Accélérateur National d'Ions Lourds (GANIL), Caen, France. A 75-MeV/nucleon ^{58}Ni^{26+} beam, on average $\approx 7 \cdot 10^{11}$ ions/s, impinged on a 660 µm thick beryllium target. Fragments were selected and identified event-by-event by the LISE3 spectrometer [24], set to optimize transmission of ^{54}Ni in its 10^+ isomeric state. The secondary beam, including $\approx$ 56% ^{54}Ni, was directed toward ACTAR TPC, within which the recoils were stopped in a gas mixture of 95% argon and 5% tetrafluoromethane at 900 mbar pressure. Any heavy ion passing a detector in front of ACTAR TPC, at an average rate of about 90/s, triggered the data acquisition system, which registered data from the LISE3 tracking and ion-identification detectors as well as 10-µs long traces of all active ACTAR TPC detector pads [13,23].

In the offline analysis, ^{54}Ni ions were selected based on correlations between energy-loss and time-of-flight information from LISE3 detectors. Thereafter, a search for proton emission was conducted, as described in detail in Ref. [13]. Note that due to the short half-life of the isomer, incoming ^{54}Ni heavy-ion tracks and proton-emission tracks are part of the same digitized ACTAR TPC event. In fact, the decay time of a single proton-emission event can be determined by evaluating the time difference between the end of the ion track and the beginning of the proton track. The proton track length is derived from a three-dimensional fit of the pad-signal distribution [13,25]. Converting the track lengths into proton-energy spectra, two well-separated peaks arise, corresponding to known $E_{p1} = 1197.9(44)$ keV and $E_{p2} = 2500.2(43)$ keV [14,26,27]. In the concluding analysis step, the observed number of counts in the peaks, $N_{p1} = 1411(40)$ and $N_{p2} = 1459(40)$, were corrected for detection efficiency by means of comprehensive Monte-Carlo simulations [13,23]. This procedure provides the branching ratio of the two proton-emission lines, which combined with the known ratio between electromagnetic decays and branch p_1 [14] yields $br_{p1} = 28.4(13)\%$, $br_{p2} = 21.1(16)\%$ and $br_{\gamma+IC} = 50.5(23)\%$ [13], as well as $T_{1/2}(10^+)_{\gamma+IC} = T_{1/2}(10^+)/br_{\gamma+IC} = 307(15)$ ns. IC denotes internal conversion.

The physics of the high-ℓ proton-emission branches from the 10^+ isomer in ^{54}Ni are subject of Ref. [13]. Here, an update and complement of isospin-symmetry (breaking) aspects are presented. The relevant experimental numbers for the $A = 54$, $T_z = \pm 1$ mirror pair are summarized in Table 1, which is an update of Table I in Ref. [14]. For completeness, Table 1 also includes $B(E2; 2^+ \rightarrow 0^+)$ values derived from relativistic Coulomb excitation measurements on ^{54}Ni [28,29].

Shell-model calculations employing the full fp shell and exploring various isospin-breaking terms are confronted with the updated experimental results provided in Fig. 1 and Table 1. For all calculations, the shell-model code ANTOINE [32,33] was used. While the main body of calculations was produced with the, at present, commonly used interactions GXPF1A [34] and KB3G [35,36], some tests were also conducted with KB3 [37,38] as well as the more recent KB3GR [39] and older FPD6 [40] empirical interactions. Electromagnetic decay properties were derived using bare g factors for $M1$ transitions and moments, as well as $E2$ effective charges of $\varepsilon_\pi = 1.15e$ and $\varepsilon_\nu = 0.80e$ for protons and neutrons, respectively [11]. Experimental γ-ray energies were used to compute transition strengths and, in case applicable, to deduce branching and mixing ratios of the transitions, and lifetimes of the nuclear states.

For mass $A = 54$ nuclei it is feasible to conduct unrestricted calculations in the fp model space. However, due to the large number

Table 1
Selected experimental results [13–15,19,28,29] and predictions from $t = 6$ fp shell-model calculations for ^{54}Fe and ^{54}Ni, employing the GXPF1A, KB3G, and KB3G56 interactions and the isospin breaking terms V_{CM}, $V_{C\ell s}$, V_{Cr}, and $V_{B:2}$ (see text for definitions and details). The experimental numbers of ^{54}Ni take into account the measured proton-emission branches from the 10^+ isomer [13], i.e., $b_{\gamma+IC} = 50.5(23)\%$ and $T_{1/2} = 155(3)$ ns are used. $B(E2)$ and $B(E4)$ values are in Weisskopf units, W.u. The calculations use free g factors, $\varepsilon_\pi = 1.15$ and $\varepsilon_\nu = 0.80$ for electric quadrupole [11], and $\varepsilon_\pi = 1.40$ and $\varepsilon_\nu = 0.30$ (this work) for hexadecapole operators, respectively.

observable	^{54}Fe				^{54}Ni			
	exp	GXPF1A	KB3G	KB3G56	exp	GXPF1A	KB3G	KB3G56
$B(E2; 2^+ \to 0^+)$	11.1(3)	9.84	7.82	8.96	10.0(19)	8.06	5.93	7.22
$B(E2; 6^+ \to 4^+)$	3.25(5)	3.01	2.84	2.99	–	2.39	2.27	2.43
$B(E2; 10^+ \to 8^+)$[a]	1.70(3)	1.92	2.12	2.15	1.91(10)	1.84	2.13	2.21
$B(E4; 10^+ \to 6^+)$	0.80(9)	0.85	0.71	0.76	4.42(98)	4.33	3.94	4.04
$br_{\gamma+IC}(10^+ \to 6^+)$	1.8(2)	1.9	1.4	1.5	5.1(11)	5.9	4.7	4.6
$T_{1/2}(10^+)_{\gamma+IC}$ (ns)	364(7)	360	327	323	307(15)	360	315	303
$Q(10^+)$ (efm^2)	52(8)[b]	60.6	55.3	56.7	–	63.6	58.3	59.5
$\mu(10^+)$ (μ_N^2)	7.281(10)	7.24	6.80	6.82	–	3.92	4.26	4.24
$E_x(10^+)$ (keV)	6527.1(11)	5954	6701	6505	6457.4(9)	5887	6596	6410

[a] Including calculated conversion coefficients of $\alpha_{\rm tot} = 0.1145(4)$ and $\alpha_{\rm tot} = 0.1350(4)$ for ^{54}Fe and ^{54}Ni, respectively [30].
[b] Using the revised $Q(3/2^-)$ of ^{57}Fe [31] as reference value.

of diagonalizations with different isospin-breaking terms, and to allow for a consistent extension towards heavier nuclei or non-yrast structures (see, e.g., [41]), the majority of calculations employed a truncation scheme allowing for an excitation of up to six nucleons from the $f_{7/2}$ shell into the upper fp shell. The latter is composed of the $p_{3/2}$, $p_{1/2}$, and $f_{5/2}$ orbitals. The notation for this truncation is '$t = 6$'. Such a truncation scheme is well established: for instance, in an early study of yrast structures in $A = 50$, $A = 51$, and $A = 52$ nuclei [35], or to explain a deformed band in ^{56}Ni [42]. Nevertheless, the validity of the $t = 6$-approach was controlled for the present study by comparing calculations with different truncation schemes ($t = 2$, $t = 4$, $t = 6$, $t = 8$, $t = 10$) with unrestricted calculations, here on behalf of the GXPF1A interaction and energy levels (cf. Fig. 1, Supplemental Material) as well as selected electromagnetic decay properties (cf. Table 1, Supplemental Material) of the main yrast cascade of ^{54}Fe [15,41]. Clearly, the variation of predictions using $t \geq 6$ for a given interaction (here: GXPF1A) is much smaller than variations between predictions based on different interactions. A relevant side note concerns the predicted energies of the core-excited $I > 6$ yrast states in ^{54}Fe: GXPF1A underestimates them by a few hundred keV, while KB3G overestimates them by a few hundred keV, likewise KB3GR and FPD6. This indicates that none of the commonly used fp-shell interactions correctly describes the gap size in the $A = 54$ mirror nuclei of interest. Thus, experimental information on the respective core-excited states, and in particular the 10^+ mirror isomers in ^{54}Fe and ^{54}Ni, carry the potential to study and adjust shell-model parameters in the future.

Isospin-breaking terms have to be incorporated into the shell-model calculations to study differences in excitation energies, so-called mirror energy differences (MED), and electromagnetic moments and decay characteristics of mirror nuclei. Thus, the fp shell-model interactions were modified according to the prescriptions of Refs. [1,3] and Ref. [4], respectively. Accounting for Coulomb multipole matrix elements, V_{CM}, of proton-proton two-body matrix-elements (TBME) as well as modifying proton and neutron single-particle energies (SPE) due to the electromagnetic spin-orbit interaction, $V_{C\ell s}$, are common. Further, Refs. [1–3] suggest to include orbit-orbit SPE corrections, $V_{C\ell\ell}$. Near closed shells, however, this term is in essence masked by radial effects related to differences in proton *minus* neutron occupation numbers between the excited state and the ground state [4], often referred to as the Thomas-Ehrman shift. Based on known excited-state energies in the ^{57}Ni-^{57}Cu mirror pair, proton SPE modifications of $V_{Cr}(p_{3/2}) = -300$ keV, $V_{Cr}(p_{1/2}) = -475$ keV, and $V_{Cr}(f_{5/2}) = -210$ keV were deemed adequate [4]. In case one considers $V_{C\ell\ell}$, then $V'_{Cr} = V_{Cr} - 100$ keV for p orbitals provides comparable results (see below). An ad-hoc solution to adjust the KB3G gap size at particle numbers $N = Z = 28$ is to increase $f_{7/2}$ SPE by 300 keV [43]. These calculations carry the label KB3G56. (See also Table 2, Supplemental Material.)

An alternative approach, originally introduced to account for differences in quadrupole deformation between ground and excited states in the middle of the $f_{7/2}$ shell [1,3], introduced an orbital-dependent strength parameter, α, to be multiplied by the difference of *total* proton and neutron $p_{3/2}$ occupation numbers between ground and excited states. With the recent advent of experimental data on even-even $A \geq 56$ mirror nuclei, strength parameters for the $p_{3/2}$ *and* $p_{1/2}$ orbitals have become subject to more detailed investigations (see Ref. [9] and references therein). To evaluate this approach at $A = 54$, $\alpha = 200$ keV is used for both p orbitals in the present study, denoted V_{Cp3} and V_{Cp1} as well as V_{Cp} for the sum of both. Note that this correction has to be inferred "by hand" after any diagonalization.

In all early MED studies (see Refs. [1,3,4] and references therein), one identified the need to include an isospin-symmetry breaking isovector term, V_B, to describe experimental data. At first, this was introduced as the "$J = 2$ anomaly" with $V_{B:2} = +100$ keV to the $f_{7/2}$ proton-proton $J = 2$ TBME. For mirror nuclei across but *within* the $f_{7/2}$ shell, using $V_{B:0} = -V_{B:2}$ was found to give similar results [5]. However, the core-excited 8^+ and 10^+ states of the $A = 54$ pair were not included in that study, though their MED rather pointed to $V_{B:2} = +100$ keV than $V_{B:0} = -100$ keV [14]. In the present work, these two terms are studied, as well as a J-dependent result, $V_{B:J}$, highlighted in Ref. [5] (see their Table II), and using -70 keV for the $J = 0$ proton-proton TBME of *all* fp orbitals, $V_{B:4x0}$, in line with Ref. [9].

For completeness, an empirical isotensor isospin-non-conserving interaction was accounted for as well [1,44]. Except for the p-orbital occupation number corrections (see above), the results always refer to fully diagonalized calculations.

The results of the present MED study are summarized in Fig. 2. Beginning with the outcome, panel (e) shows the comparison of the experimental data points with predictions based on different interactions, but the same combination of isospin-symmetry breaking terms, namely V_{CM}, $V_{C\ell s}$, V_{Cr}, and $V_{B:2}$. Independent of the underlying interaction, excellent agreement is achieved, *including* the core-excited 8^+ and 10^+ states, in line with Ref. [14].

With a focus on the KB3G interaction, panel (a) illustrates the typical rise in MED due to V_{CM}, following the alignment of a pair of nucleons in the $f_{7/2}$ shell, and remaining at $\approx +100$ keV for the core excited states. For the 0^+-6^+ states, (differences in) small occupation numbers of nucleons lead to expectedly negligible $V_{C\ell s}$ and $V_{C\ell\ell}$ contributions. This, however, changes drastically for the core-excited states, closing in to $\approx +100$ keV for each of these two single-particle effects. In order to reach the observed

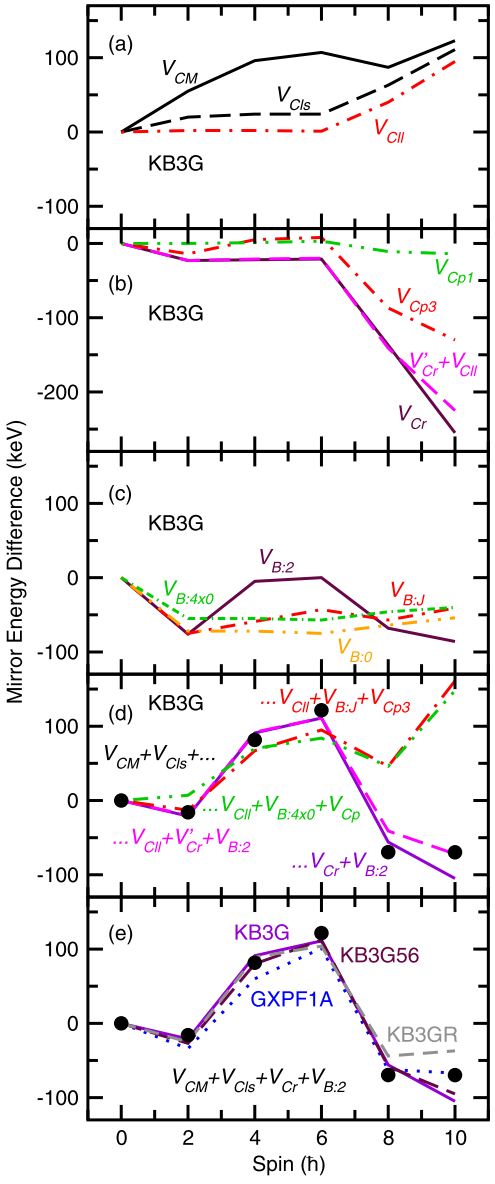

Fig. 2. Various sets of mirror-energy differences (MED) between excited states in ^{54}Ni and ^{54}Fe. Panels (a)-(d) are based on the KB3G interaction. Panel (a) provides the effect of V_{CM} (solid line), $V_{C\ell s}$ (long-dashed), and $V_{C\ell\ell}$ (dot-dashed). Panel (b) shows V_{Cr} (solid line), V'_{Cr} plus $V_{C\ell\ell}$ (long-dashed), and corrections based on $1p$-orbital occupation; V_{Cp3} (dot-dashed) and V_{Cp1} (dot-dot-dashed). Panel (c) illustrates the effects of $V_{B:2}$ (solid line), $V_{B:J}$ (dot-dashed), $V_{B:0}$ (dot-dot dashed), and $V_{B:4\times0}$ (thin dot-dot dashed). Panel (d) provides sums relevant for the discussion of isospin-symmetry breaking terms and compares these with the experimental values (filled circles, cf. Fig. 1). Panel (e) show the results for KB3G (solid line), KB3G56 (long-dashed), KB3GR (dashed), and GXPF1A (dotted), using the same combination of isospin-symmetry breaking terms, namely V_{CM}, $V_{C\ell s}$, V_{Cr}, and $V_{B:2}$. See text for definitions of these terms.

MED $= -70$ keV for the 10^+ isomer, the large positive sums of MED ≈ 200 keV ($V_{CM} + V_{C\ell s}$), or ≈ 300 keV including $V_{C\ell\ell}$, must be compensated primarily by radial effects, which are provided in panel (b).

Occupation numbers for particles in the $p_{1/2}$ orbitals are small for all states considered (< 0.15). Thus, V_{Cp1} contributions are of minor relevance. Occupation numbers for particles in the $p_{3/2}$ orbitals approach 1 for the core-excited states, giving rise to a sizable V_{Cp3} contribution of ≈ -130 keV for the 10^+ state. The V_{Cr} term catches the occupation of upper-fp-shell orbitals as well. It yields a large contribution of ≈ -260 keV. As noted earlier, the effect of $V_{C\ell\ell}$ can essentially be compensated for by $V'_{Cr} = V_{Cr} - 100$ keV

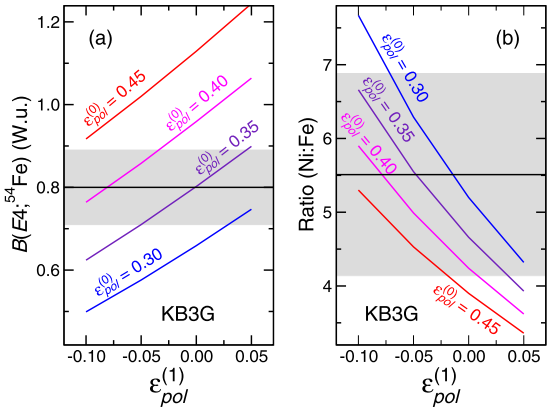

Fig. 3. (a) Reduced $B(E4; 10^+ \to 6^+)$ transition strengths of ^{54}Fe and (b) their ratios, R(Ni:Fe), as a function of the isovector polarization charge, $\varepsilon^{(1)}_{pol}$. Experimental values are indicated by the horizontal line and their uncertainties as gray regions. Predictions are plotted for different sets of isoscalar polarization charges, $\varepsilon^{(0)}_{pol}$, here based on the KB3G-plus-ISB parametrization, cf. Fig. 2(e).

for p orbitals: The respective lines in panel (b) [and panel (d)] are close and practically indistinguishable.

The different approaches to handle the isospin-symmetry breaking isovector term, V_B, are plotted in panel (c). By default, all provide the drop in MED between the 0^+ and 2^+ states. Thereafter, the more recently proposed $V_{B:0}$, $V_{B:J}$ [5], and $V_{B:4x0}$ [9] remain similar, contributing at a level of MED ≈ -50 to -70 keV. At variance [14], $V_{B:2}$ provides distinct plateaus at MED ≈ 0 keV for the 4^+ and 6^+ states, and at MED ≈ -80 keV for the core-excited states.

The sums of contributions for different approaches are provided in panel (d). Clearly, the combination of V_{CM}, $V_{C\ell s}$, V_{Cr}, and $V_{B:2}$ [4,14], as well as replacing V_{Cr} with $V'_{Cr} + V_{C\ell\ell}$, is in excellent agreement with experiment. In turn, trying to account for radial effects by parametrizing p-orbital occupation numbers [5,9] fails to describe the core-excited states in the $T_z = \pm 1$, $A = 54$ mirror system. While increasing the respective parameter to (an unrealistically large) $\alpha = 500$ keV can bend the curves down to the experimental values for the 8^+ and 10^+ states [without affecting the low-spin states, cf. panel (b)], the necessity of requiring very different α parameters to describe experimental data for even-even mass $A = 54$, $A = 56$, and $A = 58$ mirror pairs is unsatisfactory. Given the survey in panel (e), it is unlikely that using any other fp-shell interaction would alter the pattern. For validation, corresponding figures based on other fp-shell interactions are part of the Supplemental Material.

With the observation of the complete proton-emission pattern of the 10^+ isomeric state in ^{54}Ni, an experimental $B(E4; 10^+ \to 6^+) = 4.42(98)$ W.u. can be extracted. The ratio between this and the analogue transition in ^{54}Fe, $B(E4; 10^+ \to 6^+) = 0.80(9)$ W.u., becomes $R = 5.5(14)$. The constraints set by these three numbers can be used to estimate effective charges for $B(E4)$ transitions near $N = Z$, ^{56}Ni, similar to procedures outlined in Refs. [11,12]. Fig. 3 shows (a) the absolute $B(E4)$-value for ^{54}Fe and (b) the ratio, R(Ni:Fe), respectively, as a function of the isovector charge, $\varepsilon^{(1)}_{pol}$, and for different isoscalar charges, $\varepsilon^{(0)}_{pol}$. For KB3G, and likewise the other interactions of interest (cf. Table 1) and including isospin-breaking terms according to Fig. 2(e), it is found that experimental values can overall be best met with $\varepsilon^{(0)}_{pol} = 0.35(5)$ and $\varepsilon^{(1)}_{pol} = -0.05(5)$. Since $\varepsilon_\pi = 1 + \varepsilon^{(0)}_{pol} - \varepsilon^{(1)}_{pol}$ and $\varepsilon_\nu = \varepsilon^{(0)}_{pol} + \varepsilon^{(1)}_{pol}$, this implies $\varepsilon_\pi \approx 1.40$ and $\varepsilon_\nu \approx 0.30$ for $B(E4)$ transitions near ^{56}Ni.

Using the latter result (or standard effective charges, cf. [45]) to calculate the $B(E4; 2^+ \to 6^+)$ transition strength in ^{52}Mn and the $B(E4; 19/2^- \to 11/2^-)$ transition strength in ^{53}Fe the pre-

dictions exceed the measured values [46,47] by about a factor of five. This discrepancy increases to a factor of about 30 for the $B(E4; 12^+ \rightarrow 8^+)$ transition strengths in $N = Z$ ^{52}Fe [45]. A difference between the states engaged in these transitions and the ones in the $A = 54$, 10^+ isomers is that the former are all dominated by $f_{7/2}$-hole configurations, while the initial states for the latter are core excited. Below ^{100}Sn, $E4$ decays from core-excited 12^+ and 19^+ states are known in ^{98}Cd [48,49] and ^{96}Ag [49,50], respectively. Using standard effective charges, large-scale shell-model predictions reproduce the measured $B(E4; 19^+ \rightarrow 15^+)$ in ^{96}Ag but underestimate the $B(E4; 12^+ \rightarrow 8^+)$ in ^{98}Cd, though less with a less truncated model space [48,49]. Another, theoretical line of thought is the study and use of orbital or state-dependent effective operators (see, e.g., Refs. [51,52]).

To summarize, with proton radioactivity competing with electromagnetic decays of the 6457-keV, 10^+, $T_{1/2} = 155(3)$-ns isomeric state of ^{54}Ni firmly established [13], extended studies of isospin-symmetry breaking near doubly magic ^{56}Ni became accessible, relying on shell-model calculations in the full fp shell. Mirror-energy studies of the $T_z \pm 1$, $A = 54$ nuclei show that the 8^+ and 10^+ states are anchor points to assess size and validity of different approaches concerning the inclusion of isospin-symmetry breaking terms. More insights through further experimental constraints can be gained by trying to identify the low-spin non-yrast states in ^{54}Ni by means of a high-statistics, high-resolution nucleon removal reaction, by identifying states above the 10^+ states by relativistic Coulomb excitation of an isomeric ^{54}Ni beam, by measuring the lifetime of the 6^+ state expected at $\tau \approx 1.5$ ns, or by determining the magnetic moment of the isomer, $\mu(10^+) \approx 4.0\ \mu_N^2$. Finally, experimentalists may point out that all of the commonly used, present-day fp-shell interactions have deficiencies in reproducing one or the other observable of the $A = 54$, $T_z \pm 1$ mirror nuclei to full satisfaction.

Declaration of competing interest

The authors declare that they have no known competing financial interests or personal relationships that could have appeared to influence the work reported in this paper.

Acknowledgements

We are grateful to the ion-source and accelerator staff at GANIL for the provision of a stable, high-intensity, primary ^{58}Ni beam. This work was supported by the following Research Councils and Grants: European Union's Horizon 2020 Framework research and innovation programme 654002 (ENSAR2); Swedish Research Council (Vetenskapsrådet, VR 2016-3969). B.M. was an International Research Fellow of the Japanese Society for the Promotion of Science. G.F.G. acknowledges the support of the Natural Sciences and Engineering Research Council of Canada (NSERC).

Appendix A. Supplementary material

Supplementary material related to this article can be found online at https://doi.org/10.1016/j.physletb.2022.137144.

References

[1] A.P. Zuker, S.M. Lenzi, G. Martínez-Pinedo, A. Poves, Phys. Rev. Lett. 89 (2002) 142502.
[2] J. Duflo, A.P. Zuker, Phys. Rev. C 66 (2002) 051304(R).
[3] M.A. Bentley, S.M. Lenzi, Prog. Part. Nucl. Phys. 59 (2007) 497–561.
[4] J. Ekman, C. Fahlander, D. Rudolph, Mod. Phys. Lett. A 20 (2005) 2977–2992.
[5] M.A. Bentley, S.M. Lenzi, S.A. Simpson, C.Aa. Diget, Phys. Rev. C 92 (2015) 024310.
[6] J. Bonnard, S.M. Lenzi, A.P. Zuker, Phys. Rev. Lett. 116 (2016) 212501.
[7] P.J. Davies, M.A. Bentley, T.W. Henry, E.C. Simpson, et al., Phys. Rev. Lett. 111 (2013) 072501.
[8] C. Langer, F. Montes, A. Aprahamian, D.W. Bardayan, et al., Phys. Rev. Lett. 113 (2014) 032502.
[9] A. Fernández, A. Jungclaus, P. Doornenbal, M.A. Bentley, et al., Phys. Lett. B 823 (2021) 136784.
[10] N. Michel, W. Nazarewicz, M. Płoszajczak, Phys. Rev. C 82 (2010) 044315.
[11] R. du Rietz, J. Ekman, D. Rudolph, C. Fahlander, et al., Phys. Rev. Lett. 93 (2004) 222501.
[12] H. Grawe, K. Straub, T. Faestermann, M. Górska, et al., Phys. Lett. B 820 (2021) 136591.
[13] J. Giovinazzo, T. Roger, B. Blank, D. Rudolph, et al., Nat. Commun. 12 (2021) 4805.
[14] D. Rudolph, R. Hoischen, M. Hellström, S. Pietri, et al., Phys. Rev. C 78 (2008) 021301(R).
[15] Yang Dong, Huo Junde, Nucl. Data Sheets 121 (2014) 1–142.
[16] I. Reusen, A. Andreyev, J. Andrzejewski, N. Bijnens, et al., Phys. Rev. C 59 (1999) 2416–2421.
[17] M.J. López Jiménez, B. Blank, M. Chartier, S. Czajkowski, et al., Phys. Rev. C 66 (2002) 025803.
[18] A. Gadea, S.M. Lenzi, S. Lunardi, N. Mărginean, et al., Phys. Rev. Lett. 97 (2006) 152501;
A. Gadea, S.M. Lenzi, S. Lunardi, N. Mărginean, et al., Phys. Rev. Lett. 97 (2006) 199901 (Erratum).
[19] E. Dafni, J.W. Noé, M.H. Rafailovich, G.D. Sprouse, Phys. Lett. B 76 (1978) 51–53.
[20] K. Stahl, A. Wendt, P. Reiter, D. Rudolph, et al., Eur. Phys. J. A 56 (2020) 22–30.
[21] T. Roger, J. Pancin, G.F. Grinyer, B. Mauss, et al., Nucl. Instrum. Methods Phys. Res., Sect. A 895 (2018) 126–134.
[22] B. Mauss, P. Morfouace, T. Roger, J. Pancin, et al., Nucl. Instrum. Methods Phys. Res., Sect. A 940 (2019) 498–504.
[23] J. Giovinazzo, et al., submitted to Nucl. Instrum. Methods Phys. Res., Sect. A.
[24] R. Anne, A.C. Mueller, Nucl. Instrum. Methods Phys. Res. B 70 (1992) 276–285.
[25] J. Giovinazzo, J. Pancin, J. Pibernat, T. Roger, Nucl. Instrum. Methods Phys. Res., Sect. A 953 (2020) 163184.
[26] A. Kankainen, V.-V. Elomaa, T. Eronen, D. Gorelov, et al., Phys. Rev. C 82 (2010) 034311.
[27] P. Zhang, X. Xu, P. Shuai, R.J. Chen, et al., Phys. Lett. B 767 (2017) 20–24.
[28] K.L. Yurkewicz, D. Bazin, B.A. Brown, C.M. Campbell, et al., Phys. Rev. C 70 (2004) 054319.
[29] K. Yamada, T. Motobayashi, N. Aoi, H. Baba, et al., Eur. Phys. J. A 25 (2005) 409–413.
[30] T. Kibédi, T.W. Burrows, M.B. Trzhaskovskaya, P.M. Davidson, C.W. Nestor Jr., Nucl. Instrum. Methods Phys. Res., Sect. A 589 (2008) 202–229.
[31] G. Martínez-Pinedo, P. Schwerdtfeger, E. Caurier, K. Langanke, W. Nazarewicz, T. Söhnel, Phys. Rev. Lett. 87 (2001) 062701.
[32] E. Caurier, Shell Model Code ANTOINE, IRES Strasbourg, 1989–2002.
[33] E. Caurier, F. Nowacki, Acta Phys. Pol. 30 (1999) 705–714.
[34] M. Honma, T. Otsuka, B.A. Brown, T. Mizusaki, Phys. Rev. C 65 (2002) 061301(R).
[35] A. Poves, J. Sánchez-Solano, E. Caurier, F. Nowacki, Nucl. Phys. A 694 (2001) 157–198.
[36] E. Caurier, G. Martinez-Pinedo, F. Nowacki, A. Poves, A.P. Zuker, Rev. Mod. Phys. 77 (2005) 427–488.
[37] A. Poves, A.P. Zuker, Phys. Rep. 70 (1981) 235–314.
[38] T.T.S. Kuo, G.E. Brown, Nucl. Phys. A 114 (1968) 241–279.
[39] E. Caurier, A. Poves, unpublished.
[40] W.A. Richter, M.J. Van Der Merwe, R.E. Julies, B.A. Brown, Nucl. Phys. A 523 (1991) 325–353.
[41] D. Rudolph, I. Ragnarsson, C. Andreoiu, M.A. Bentley, et al., Phys. Rev. C 102 (2020) 014316.
[42] D. Rudolph, C. Baktash, M.J. Brinkman, E. Caurier, et al., Phys. Rev. Lett. 82 (1999) 3763.
[43] D. Rudolph, C. Andreoiu, M.A. Bentley, M.P. Carpenter, et al., Phys. Rev. C 104 (2021) 044314.
[44] S.M. Lenzi, M.A. Bentley, R. Lau, C.Aa. Diget, Phys. Rev. C 98 (2018) 054322.
[45] A. Gadea, S.M. Lenzi, D.R. Napoli, M. Axiotis, et al., Phys. Lett. B 619 (2005) 88–94.
[46] R.P. Yaffe, R.A. Meyer, Phys. Rev. C 16 (1978) 1581.
[47] J.N. Black, Wm.C. McHarris, W.H. Kelly, B.H. Wildenthal, Phys. Rev. C 11 (1975) 939.
[48] A. Blazhev, M. Górska, H. Grawe, J. Nyberg, et al., Phys. Rev. C 69 (2004) 064304.
[49] J. Park, R. Krücken, D. Lubos, R. Gernhäuser, et al., Phys. Rev. C 96 (2017) 044311.
[50] P. Boutachkov, M. Górska, H. Grawe, A. Blazhev, et al., Phys. Rev. C 84 (2011) 044311.
[51] H. Sagawa, B.A. Brown, Phys. Lett. B 150 (1985) 247–252.
[52] R. Hoischen, D. Rudolph, H.L. Ma, P. Montuenga, et al., J. Phys. G, Nucl. Part. Phys. 38 (2011) 035104.